Available online at www.sciencedirect.com

ScienceDirect

ARTICLE

Effects of Trace Reinforcements on Microstructure of TC18 Titanium Matrix Composite

Sun Shuyu[1],   Lv Weijie[2]

[1] Taizhou University, Taizhou 318000, China; [2] State Key Laboratory of Metal Matrix Composites, Shanghai Jiao Tong University, Shanghai 200240, China

Abstract: Ti-5Al-5Mo-5V-1Fe-1Cr titanium matrix composites reinforced with different mass fractions of TiB and TiC were fabricated via a consumable vacuum arc-remelting furnace. The reinforcements can significantly refine β phase during heat treatment. However, the extent of the microstructure refinement decreases gradually with the increase of the reinforcements. It is revealed that the microstructural phenomenon is associated with Zener dragging force exerted by the reinforcements. The increase rate of the dragging force tends to decrease with the increase of the reinforcements. Additionally, the effects of the reinforcements on the spheroidization of α were also investigated. The spheroidization rate of α fluctuates somewhat with increasing the trace reinforcements during heat treatment. Nevertheless, the reinforcements accelerate the spheroidization of α lath in the Widmannstatten structure obviously during isothermal compression. The effects of the reinforcements during isothermal compression are different from those during heat treatment. In addition to accelerating the diffusion significantly, the trace reinforcements also contribute to the spheroidization of α by accelerating interface transformation during isothermal compression.

Key words: TC18 Ti matrix composite; trace reinforcement; spheroidization of α; refinement of β

In situ synthesized composites reinforced with TiB fibers and TiC particles have been attracting considerable attention in recent years[1-3]. Ti-5Al-5Mo-5V-1Fe-1Cr (TC18) titanium alloy is an important aviation material. A tendency of α spheroidization appears when the annealing temperature is lower than the phase transformation temperature[4]. In order to refine microstructure and improve mechanical properties of the alloy, TC18 titanium matrix composites (TMCs) reinforced with trace TiB and TiC are fabricated. The experiments show that the spheroidization rate of α fluctuates somewhat with increasing the reinforcements during heat treatment. Nevertheless, the trace reinforcements accelerate the spheroidization of α lath in the α/β colony structure during isothermal compression. Little information is available to date concerning the effects of reinforcements on the spheroidization of α lath in the α/β colony structure. Reinforcements can refine β phase in TMC by exerting Zener dragging force[5,6]. However, the extent of the microstructure refinement decreases gradually with the increase of the reinforcements during heat treatment.

The aim of the present paper is to study the effects of the mass fraction of trace reinforcements on the grain growth during heat treatment and the effects of trace reinforcements on the spheroidization of α lath during isothermal compression, so as to provide valuable technical information for further research and development of TC18 TMC.

1   Experiment

The stoichiometric mass fractions of the raw materials including sponge Ti, B_4C powder, Al, Al-Mo, Al-V, Fe and Cr were blended uniformly, and then were compacted into pellets. The pellets were melted in a consumable vacuum arc-remelting furnace. Small addition of B_4C (0.4 wt%) to Ti produced TiB and TiC during solidification by a chemical reaction: $5Ti + B_4C = 4TiB + TiC$. The mass fractions of the reinforcements in the composites are provided in Table 1. The

phase transformation temperature of the ingot of TMC3 is 885 ℃.

The as-cast ingots were then forged at 1150 ℃ and rolled at 840 ℃ into rods with the diameter of 15 mm. Phase identifications indicate that there are three kinds of phases in the composites, Ti, TiB and TiC. In order to control the overgrowth of grains and obtain good mechanical properties, we employed triplex heat treatment procedures as follows: (1) heat treatment A (HTA): 860 ℃/1.5 h + FC, 750 ℃/1.5 h+AC, 600 ℃/4 h + AC; (2) heat treatment B (HTB): 910 ℃/1.5 h +FC, 750 ℃/1.5 h +AC, 600 ℃/4 h +AC.

Anti-oxidation coating was used during heat treatment. TC18 Ti alloy was also prepared with the same method. The raw materials did not contain B_4C. The phase transformation temperature of the alloy is 865 ℃.

For tensile testing, 30 mm gage length cylindrical speci-mens (6 mm in diameter) were machined from the rods undergoing HTA treatment. Tensile tests were conducted with a strain rate of 0.001 s^{-1}. Subsequently, isothermal compression tests were conducted on a Gleeble simulator. The cylindrical specimens with the diameter of 8 mm and the height of 12 mm were machined from the rods undergoing HTB treatment. After the compression, the specimens were water quenched immediately.

Microstructure observations by optical microscope (OM), and scanning electron microscope (SEM) were conducted after the polishing and etching. Moreover, transmission electron microscope (TEM) was also used.

2 Results and Discussion

2.1 Spheroidization of α during heat treatment

Fig.1 shows SEM microstructure of the specimens undergoing HTA treatment. The phase contrast of α in SEM images is black. Primary α dispersing in β phase is as nearly equiaxed, plate-shaped and rod-shaped. Nevertheless, primary α tends to be spheroidized. The microstructure inhomogeneity in Fig.1 is associated with the segregation.

Fig.2a shows the selected area electron diffraction (SAED) patterns of α and β grains in TMC3 undergoing HTA treatment. It presents the non-coherent α/β interface. The spheroidization rates of α in the alloy, TMC1, TMC2 and TMC3 are about 28%, 33%, 32% and 35%, respectively. The spheroidization of α is determined based on an aspect ratio $l/b<2$, in which l and b denote the length and thickness of α, respectively.

EDS results in Fig.2b show that the mass fractions (wt%) of Al, Mo, Fe and Cr at point A are 2.5, 16.3, 2.8 and 3.5,

Table 1 Composites and mass fractions of reinforcements (wt%)

Specimen	B₄C addition	TiB	TiC
TMC1	0.1	0.4	0.1
TMC2	0.2	0.8	0.2
TMC3	0.4	1.6	0.4
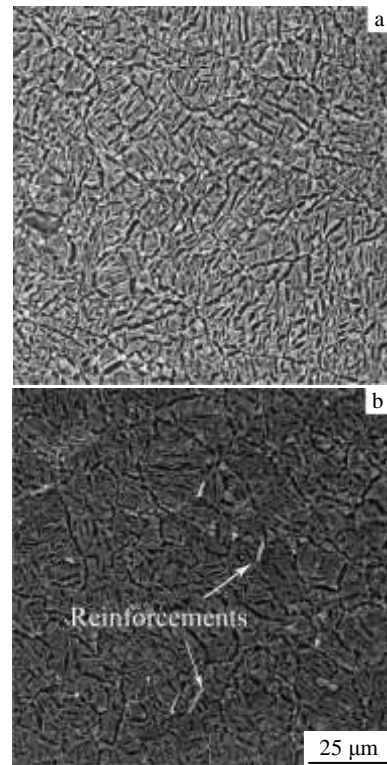
Fig.1 SEM microstructures of the specimens undergoing HTA treatment: (a) alloy and (b) TMC1
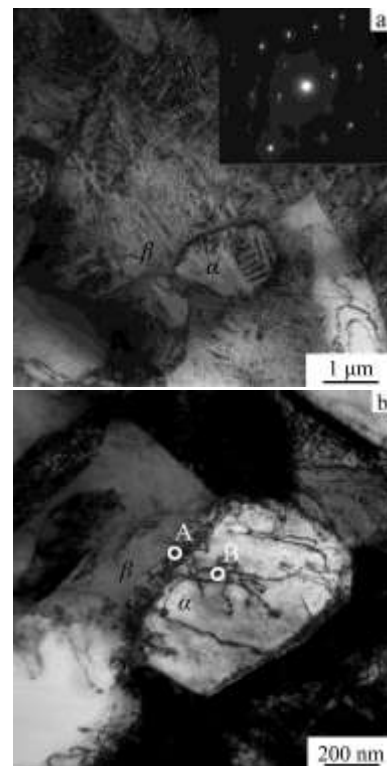
Fig.2 TEM images of TMC3 undergoing HTA treatment: (a) α, β and corresponding SAED pattern and (b) dislocations in α

respectively, while those at point B are 4.6, 4.4, 0.9 and 1.1, respectively. The atomic radii of Ti, Al, Mo, V, Fe, and Cr are 140, 125, 145, 135, 140 and 140 pm, respectively. The electro negativities of the elements are 1.5, 1.6, 1.8, 1.6, 1.8 and 1.6, respectively. The differences in the atomic radius and electro negativity cause the segregation of the elements. The equilibrium grain boundary segregation, C_{gb}, can be estimated by [7]:

$$C_{gb} = \frac{C_m A \exp(Q/RT)}{1 + C_m A \exp(Q/RT)} \quad (1)$$

where, C_m is solute concentration of elements in grain, and A is vibrational entropy factor at grain boundary. R and T are gas constant and absolute temperature, respectively. Q is difference of distortion energy between grain and grain boundary. The segregation retards the formation of Frank dislocation network in α in Fig.2b, which increases Q and C_{gb}. The boundary segregation exerts dragging force on grain boundary migration (GBM) and thus causes the anisotropy of GBM.

It only presents in-situ recrystallization in α due to the high stacking fault energy of hcp structure and high dispersivity of α[8]. Therefore, the boundary migration of α and $\beta \rightarrow \alpha$ phase transformation shares the same driving force that is chemical driving force.

On the one hand, the reinforcements increase the segregation; on the other hand, the reinforcements can promote the driving force for the boundary migration of α grain by accelerating diffusion due to the non-coherent α/β interface. Therefore, the spheroidization rate of α fluctuates somewhat with the increase of the reinforcements.

2.2 Refinement of β during heat treatment

Fig.3 shows the variation of β grain size with mass fraction of B$_4$C addition after HTA treatment. As shown in Fig.1, owing to the effects of the anti-oxidation coating, β phase decorated with boundary α can be observed after the heat treatment. The average β grain size in TMC1 decreases by more than 40% comparing with that of the alloy. However, the extent of the microstructure refinement decreases gradually with increasing the reinforcements.
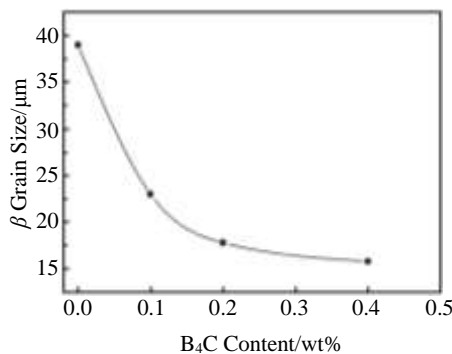
Fig.3   Variation of β grain size with mass fraction of B$_4$C addition after HTA treatment

Fig.4a shows TEM image of TiC and the corresponding SAED pattern. The distribution and morphologies of TiC are influenced mainly by the synthesis temperature. TiC particles precipitate in binary eutectic and ternary eutectic reactions growing in equiaxial shape[9]. Fig.4b shows TEM image of TiB and SAED patterns of TiB and α. The locations of boron atoms and the lattice mismatch energy between TiB and Ti matrix play key roles in the formation of stacking faults[10]. TiB fiber provides nucleation site for α in Fig.4b. The stacking faults in α are presented as interference fringe pattern.

TiB has an average length of 7.9 µm after heat treatment, while TiC 2.6 µm. The reinforcements have a wide range of size distribution, e.g. the size of TiC ranges from less than 200 nm to more than 4 µm. A broad size distribution of particles gives rise to a larger Zener dragging force than a narrow size distribution of particles[11]. Therefore, the trace reinforcements exert large Zener dragging force on the boundary migration of β grain.

The β grain sizes less than 20 µm, within 20~30 µm, within 30~40 µm, within 40~50 µm are about 12.5%, 25%, 18.75% and 21.88%, respectively. The size distributions of 10~20 µm and 20~30 µm in TMC1 are 43.75% and 46.87%, respectively. The size distribution of 10~20 µm in TMC2 is 70.3%. However, the size distribution of 10~20 µm in TMC3 is more than 90% of the total.

The size distribution of β grain becomes narrow with increasing the reinforcements. The results indicate that the rate
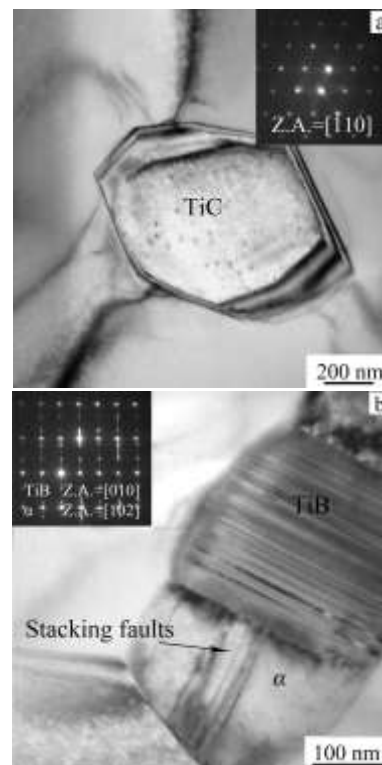
Fig.4   TEM images and corresponding SAED patterns of reinforcements TiC (a) and TiB (b)

of merging of β grains with topological defects is accelerated.

Therefore, the average boundary energy of β grain has a tendency to decrease with increasing the reinforcements. Zener drag of the reinforcements, P_r, can be assumed by:

$$P_r = \frac{3fE_H}{2r} \qquad (2)$$

where, E_H is average boundary energy of β grain, f is volume fraction of particle, and r is particle size. The decrease of E_H results in the decrease of P_r.

The result in Fig.3 is also associated with boundary α decorating β. Primary α preferentially precipitates at β grain boundaries to decrease nucleation energy during heat treatment. Therefore, the pinning effects of boundary α on the boundary migration of β grain do not linearly increase with increasing the reinforcements.

The driving force for the boundary migration of β grain is different from that of α. The growth of α increases the dislocation density in β due to the difference of the specific volume between α and β. This increases the difference of distortion energy among β grains, i.e. the driving force for GBM of β is increased. The reinforcements can accelerate the precipitation of α by providing nucleation sites for α and increasing dislocation density.

2.3 Tensile properties of the alloy and composites

Fig.5 shows room-temperature tensile properties of the alloy and the composites undergoing HTA treatment. The correlation between σ_y (yield strength) and $d^{-0.5}$ (average size of β grain) of the materials was examined. The correlation coefficient is 0.81. Therefore, in addition to the load bearing of TiB and the dispersion strengthening of TiC, the grain refinement strengthening also plays an important role in promoting the strengths of the composites.

The increase of the number of β grains and the load bearing of TiB can improve the homogeneity of the loads applied to each β grain. Thus, the refinement of β and the spheroidization of α can promote the elongation of the composites by decreasing crack initiation. During the process of the concentrated deformation, the crack-tip blunting and crack deflection caused by the reinforcements as well as the load bearing of unbroken TiB can contribute to promoting the reduction of area of the composites. However, partial increases in the strength and the plasticity of the composites are offset by the trace reinforcements[8]. Therefore, the plasticity of the composites fluctuates and tends to decrease in Fig.5.

2.4 Spheroidization of α during isothermal compression

The microstructures of the materials exhibit the characteristics of Widmannstatten structure after HTB treatment. Some randomly oriented α/β colony structures intersect each other within a prior β grain. α/β laths are oriented along preferred orientations (per Burger's orientation relationship between α and β). Fig.6a shows the microstructure of the end of the alloy

Fig.5 Tensile properties of alloy and composites undergoing heat treatment: (a) yield stress σ_y and elongation δ; (b) ultimate stress σ_b and reduction of area ψ
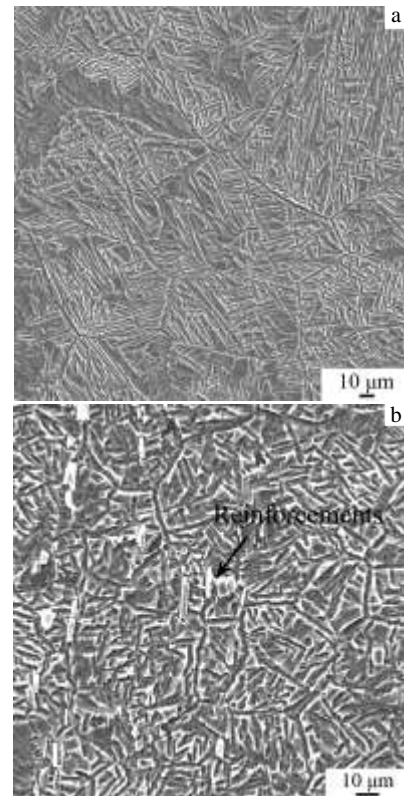
Fig.6 SEM images of specimens undergoing isothermal compression: (a) alloy and (b) TMC3

specimen after isothermal compression. The phase contrast is black; *β*, white. The compression condition is 840 ℃/0.01 s⁻¹/60% (temperature/strain rate/deformation reduction). *α*, Owing to the friction between the specimen and the push rod of the Gleeble simulator, the microstructure shows the characteristics of Widmannstatten structure. The microstructure of TC18 TMC is also refined significantly during isothermal compression. For example, the average grain sizes of the alloy are about 86 μm (840 ℃/0.01 s⁻¹/60%), 78 μm (840 ℃/0.001 s⁻¹/60%), 83 μm (840 ℃/0.001 s⁻¹/40%) and 81 μm (790 ℃/0.001 s⁻¹/60%). However, those of TMC3 are about 29 μm (840 ℃/0.01 s⁻¹/60%), 26 μm (840 ℃/0.001 s⁻¹/60%), 27 μm (840 ℃/0.001 s⁻¹/40%) and 26 μm (790 ℃/0.001 s⁻¹/60%). Fig.6b shows the microstructure of TMC3 after isothermal compression. Generally, *α* grain is divided and then is spheroidized during hot deformation. The *α*/*β* interface can change from coherent or semi-coherent interface into incoherent interface during hot deformation, which leads to the spheroidization of *α*[12-14]. Some *α* laths in the *α*/*β* colony structure are coarsened and then spheroidized in Fig.6b. The trace reinforcements accelerate the interface transformation by increasing lattice distortion, which thus accelerates the spheroidization of *α*.

The increase of temperature during isothermal compression can be assumed by[15]:

$$\Delta \theta = \frac{k_{wm} |\varphi_n|}{\rho c_p} \qquad (3)$$

where k_{wm} is average flow stress, and $|\varphi_n|$ is deformation coefficient. ρ and c_p are density and specific heat capacity, respectively. TiB has an average aspect ratio of 7.1 (length/ diameter). The fibers tend to parallel to the maximum shearing stress during isothermal compression, which promotes the load bearing effects of TiB fibers significantly. Fig.7 shows *σ-ε* curves of the alloy and TMC3 during isothermal compression. Owing to the load bearing effects of TiB fibers, the dispersion strengthening of TiC and grain refinement strengthening, the strengths of the composites are higher than that of the alloy. Thus, k_{wm} of the composite is higher than that of the alloy significantly. The deformation temperature of the composite is promoted remarkably, which accelerates the diffusion.

As shown in Fig.8, dynamic softening has an absolute advantage in the competition with work hardening. The compression condition is 840 ℃/0.01 s⁻¹/60%. This is partly attributed to the increase of the deformation temperature. The dislocation density in Fig.8b is remarkably lower than that in Fig.8a. The dislocations increase the difference of distortion energy between grain and grain boundary, which retards the spheroidization of *α*. Fig.8b shows the ongoing coalescence process of two *α* grains.

Owing to the acceleration of diffusion, the resistance on the boundary migration of *α* grain caused by the segregation is relatively easy to overcome during hot deformation.
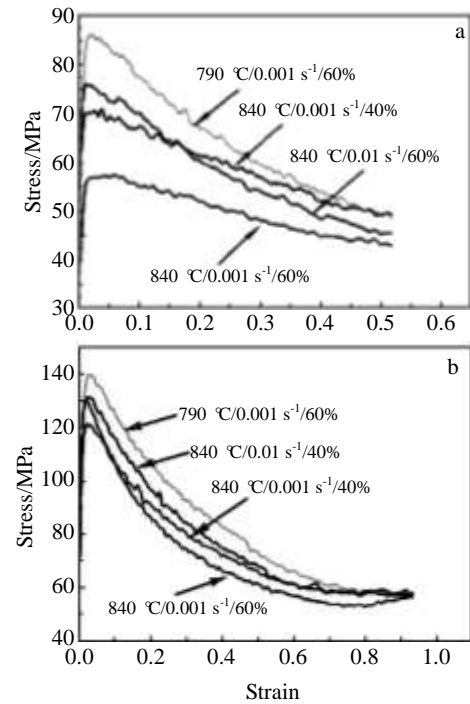
Fig.7   *σ-ε* curves during isothermal compression: (a) alloy and (b) TMC3
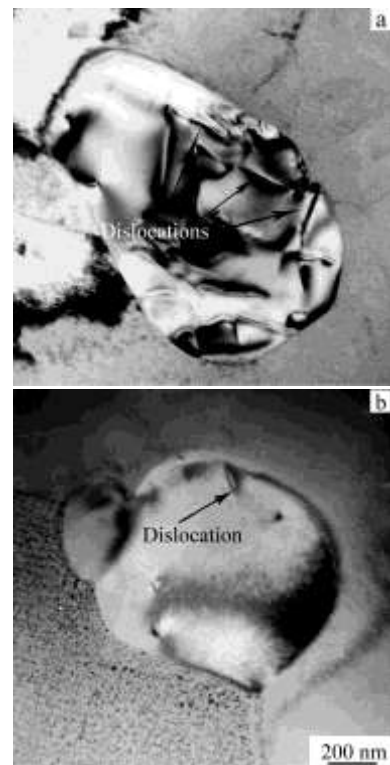
Fig.8   TEM images of TMC3 undergoing isothermal compression: (a) near elliptical *α* and (b) spheroidized *α*

3 Conclusions

1) Trace reinforcements accelerate the diffusion and increase the segregation simultaneously. Therefore, the spheroidization rate of α fluctuates somewhat with the increase of the reinforcements during heat treatment.

2) The extent of the microstructure refinement decreases gradually with increasing trace reinforcements. It is associated with Zener dragging force exerted by the reinforcements. The rate of increase of the dragging force tends to decrease with the increase of the reinforcements.

3) In addition to the acceleration of diffusion, trace reinforcements also can accelerate the spheroidization of α lath in the Widmannstatten structure by helping to change the mismatch of α/β interface during isothermal compression.

References

1 Ni D R, Geng L, Zhang J *et al. Scripta Materialia*[J], 2006, 55: 429

2 Bhat B V R, Subramanyam J, Prasad V V B. *Material Science and Engineering A*[J], 2002, 325: 126

3 Rahoma H K S, Chen Y Y, Wang X P *et al. Journal of Alloys and Compounds*[J], 2015, 627: 415

4 Sun Shuyu, Lv Weijie. *Rare Metal Materials and Engineering*[J], 2016, 45(6): 1138

5 Nes E, Ryum N, Hunderi Q. *Acta Materialia*[J], 1985, 33: 11

6 Gottstein G, Shvindlerman L S. *Scripta Materialia*[J], 2010, 63: 1089

7 Mcleand D. *Grain Boundaries in Metals*[M]. Oxford: Oxford University Press, 1957: 68

8 Sun S Y, Wang L Q, Qin J N *et al. Material Science and Engineering A*[J], 2011, 530: 602

9 Ding H, Liu X, Yu L *et al. Scripta Materialia*[J], 2007, 57: 575

10 Feng H, Zhou Y, Jia D *et al. Scripta Materialia*[J], 2006, 55: 667

11 Eivani A R, Valipour S, Ahmed H *et al. Metallurgical and Materials Transactions A*[J], 2011, 42: 1109

12 Zherebtsov S, Murzinova M, Salishchev G *et al. Acta Materialia*[J], 2011, 59: 4138

13 Furuhara T, Ogawa T, Maki T. *Philosophical Magazine Letters*[J], 1995, 72: 175

14 Zherebtsov S, Salishchev G, Semiatin S L. *Philosophical Magazine Letters*[J], 2010, 90(12): 903

15 Kopp R, Wiegels S H. *Einführung in Die Umformtechnik*[M]. Aachen: Verlag Mainz, 1999: 63

微量增强体对 TC18 钛基复合材料微观组织的影响

孙曙宇 [1]，吕维洁 [2]

(1. 台州学院，浙江 台州 318000)

(2. 上海交通大学 金属基复合材料国家重点实验室，上海 200240)

摘　要： 使用真空自耗炉制备出多种微量 TiB 和 TiC 增强的 Ti-5Al-5Mo-5V-1Fe-1Cr 钛基复合材料，增强体在热处理过程中可大幅细化 β 相，但是细化幅度却随着增强体含量的增加而变缓，文中揭示出这和增强体的 Zener 拖曳力变化有关，增强体含量增加而拖曳力增幅变缓。此外还研究了增强体对 α 相球化的作用，α 球化率随着增强体含量增加而小幅波动，然而在其作用下，等温压缩过程中魏氏体群结构中的板条状 α 明显加快了球化。等温压缩过程中，增强体对 α 球化的作用不同于热处理过程，除了显著加速扩散之外，微量增强体还可以通过促进界面转变而加速 α 相球化。

关键词： TC18 钛基复合材料；微量增强体；α 相球化；β 相细化

作者简介：孙曙宇，男，1971 年生，博士，台州学院机械学院，浙江 台州 318000，电话：0576-88661930，E-mail: sun.shuyu@126.com